Motion-enhanced magnetic moments of excitons in ZnSe

J. J. Davies,* L. C. Smith, and D. Wolverson Department of Physics, University of Bath, Bath BA2 7AY, United Kingdom

A. Gust, C. Kruse, and D. Hommel

Institute for Solid State Physics, Semiconductor Epitaxy Group, University of Bremen, D-28334 Bremen, Germany

V. P. Kochereshko

A. F. Ioffe Physico-Technical Institute, RAS, 194021 St. Petersburg, Russia (Received 2 September 2009; revised manuscript received 4 January 2010; published 9 February 2010)

Recent studies of excitons in wide quantum wells have shown that the magnetic properties are strongly affected as the excitons acquire kinetic energy. In the center of mass approximation, these motion-induced changes are ascribed to mixing between the 1S exciton ground state and the higher lying nP states. The origin of the mixing is due to the dispersion curves for the valence band not being of simple parabolic form. Detailed previous studies of excitons in CdTe have resulted in excellent agreement between experiment and the predictions of this model. One consequence of the mixing is that the magnetic moment of the exciton is not simply the sum of the magnetic moments of the electron and hole, but contains motion-induced contributions, which can easily dominate the contributions from the individual charge carriers. To confirm the validity of the model, we have carried out detailed investigations of the magnetic properties of center of mass excitons in a second semiconductor, ZnSe, for which the magneto-optical properties of the individual charge carriers are completely different from those of CdTe. Excellent agreement is obtained between theory and experiment with a choice of the Luttinger parameter γ_3 =0.98, in close agreement with the value determined independently by two-photon magnetoabsorption experiments. The success of the model when applied to both materials provides strong evidence that motion-induced changes in magnetism are a universal feature in zinc-blende semiconductors.

DOI: 10.1103/PhysRevB.81.085208 PACS number(s): 71.35.Cc, 71.35.Ji, 78.20.Ls, 78.55.Et

I. INTRODUCTION

Experiments in magnetic fields can provide considerable insight into the electronic structure of excitons. In recent papers, 1-5 we have shown that this structure becomes modified as the kinetic energy of the excitons becomes larger. To account for this, we have proposed a model² in which the exciton ground state is mixed with excited states. The origin of the mixing is due to the dispersion curves for the valence band not being of simple parabolic form. In particular, the model provides an accurate quantitative description of the extensive data for CdTe. It leads to the important conclusion that the magnetic behavior of excitons cannot be explained simply by adding together the properties of the individual constituent particles (as has often been done in the literature): in fact, for CdTe, the motion-induced contributions to the magnetism begin to dominate those of the constituent electrons and holes as the exciton kinetic energy becomes larger. The motivation behind the present work was to show that this motion-induced behavior is observed in a different semiconductor and that the model constructed for CdTe is applicable here also, thus providing strong evidence for the universality of the phenomena in zinc-blende semiconductors. ZnSe is a particularly suitable choice because (i) its band gap is much larger than that of CdTe (so that contributions to the magnetism from interband mixing are much smaller) (ii) the ZnSe exciton binding energy is much greater than that of CdTe (so that quantum confinement effects on the individual charge carriers are relatively less important), and (iii) the magnetic moments (g values) of the electrons and holes are of opposite sign to, and, therefore, completely different from, those in CdTe, so that conclusive evidence can be obtained that it is not the magnetic moments of the individual particles that matter, but that of the exciton as a whole.

The key to our approach is the confining of excitons in quantum wells whose width L is much larger than the exciton radius and in which the lowest confinement energies of the exciton are less than its binding energy. Under such circumstances, the exciton can be described with the "adiabatic" or center of mass (c.m.) approximation, 6-10 in which it is treated as a composite hydrogen-like particle in which the electron and hole orbit one another (the internal motion). In a wide quantum well of sufficient depth, the translational motion of the center of mass can be described by a wave vector K, whose component normal to the plane of the well is quantized, to a first approximation, according to $K_z = N\pi/L$, where N is a nonzero integer. If the sample quality is sufficiently high, the exciton recombination energies for states with different values of N can be resolved in photoluminescence (PL) experiments and their behavior under magnetic fields can be investigated. In particular, the Zeeman splitting, which is a measure of the exciton magnetic moment, can be studied for different values of K_Z and therefore as a function of kinetic energy. The magnetic moment itself is sensitive to the electronic structure of the exciton.

The plan of the paper is as follows. Following a description of the experimental data (Sec. II), we summarize briefly (Sec. III) the mixing process that modifies the magnetic properties. The model is applied successfully to ZnSe and our overall conclusions presented (Sec. IV).

II. EXPERIMENTAL DETAILS

A. Sample growth

Samples of ZnSe/ZnSSe with nominal well thicknesses of 20, 28, and 40 nm were grown by molecular beam epitaxy in a twin-chamber system, on top of 180 nm GaAs buffer layers on (001) GaAs substrates. The ZnSSe layer thicknesses were 1 μ m on the GaAs side and 0.5 μ m on the top side. The samples were characterized as described in Ref. 11, the well thicknesses determined by high resolution x-ray diffraction being 20.7, 29.4, and 43.7 nm, respectively. The sulfur contents in the barriers were 5.2%, 5.0%, and 5.8%, respectively, leading to barrier/well band gap differences on the order of 23–28 meV.

The specimens are strained such that the heavy-hole (HH) states lie lower than those of the light holes (LHs). At 2 K, we find that the strain contribution *S* to the energy difference between the HH and LH excitons is about 13 meV.

The well widths are more than five times the ZnSe exciton Bohr radius (\sim 3.5 nm) and the confinement energies of the excitons are smaller than the exciton Rydberg R (e.g., for the lowest exciton state, the confinement energies in the 20 nm well are on the order of an meV, compared with $R\approx$ 20 meV). ¹²

B. Photoluminescence spectra

Photoluminescence spectra for magnetic fields up to 6 Tesla were excited at 2 K by using the 325 nm line from a He-Cd laser. The angle θ between the magnetic field and the growth axis could be altered continuously between zero and 90°. Examples of the spectra for the sample with a well width of 43.7 nm are shown in Fig. 1.

The PL spectrum in zero magnetic field shows a clearly resolved set of lines whose energies can be described to a good approximation by

$$E_N = E_0 + N^2 h^2 / 8M_{HH} L^2, (1)$$

where M_{HH} is the HH exciton translational mass for motion in the growth direction, as appropriate for a particle of mass M_{HH} in wide quantum well of large depth. Figure 2 shows this dependence for all three specimens, the value of M_{HH} being 1.26 m_0 , where m_0 is the mass of a free electron. This is identical to the value obtained for ZnSe layers in Ref. 13 (where the relation between the translational mass and the Luttinger parameters¹⁴ is discussed). In the present work, the values of $K_z = N\pi/L$ for most of the transitions are in the range $(1-6) \times 10^6$ cm⁻¹ and therefore significantly greater than the magnitude of the photon wave vector k_{photon} $(\approx 0.5 \times 10^6 \text{ cm}^{-1})$ so that the relevant part of the polariton dispersion curve is close to that of a simple c.m. exciton. The data in Fig. 2 thus enable the values of N to be assigned for each specimen. A full discussion of the fit to the line positions is given in Ref. 11.

When a magnetic field $\vec{\bf B}$ is applied along the growth direction ([001], taken to be the z axis), the lines in the PL spectra split and become circularly polarized (Fig. 1). For excitons formed from electrons and heavy-holes, the optically active states $|m_J,m_s\rangle$ in this field configuration are

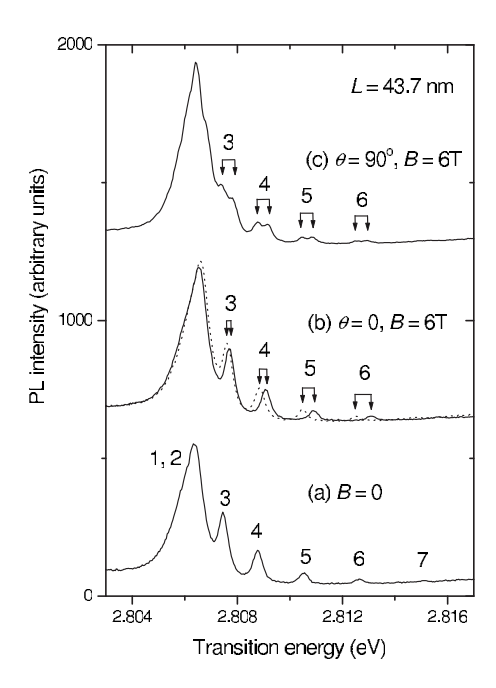


FIG. 1. PL spectra at 2 K from the specimen with well width 43.7 nm: (a) in zero magnetic field; (b) in a field of 6 T applied along the growth direction (the solid and broken lines refer, respectively, to σ_+ and σ_- polarization of the emitted light); (c) in a field of 6 T applied perpendicular to the growth direction. In cases (b) and (c), the energy splittings caused by the magnetic field are indicated by the pairs of arrows. The values of the translational quantum number N are shown.

 $|3/2,-1/2\rangle$ and $|-3/2,1/2\rangle$, where m_J and m_s are, respectively, the magnetic quantum numbers for the valence band hole and the conduction band electron. The Zeeman splitting between these states can be characterized by a parameter $g_{\rm exc}$, defined according to $E_{\sigma+}-E_{\sigma-}=g_{\rm exc}\mu_B B$ where μ_B is the Bohr magneton.

For an exciton at rest, one would expect $g_{\text{exc}} = g_{HH} - g_e$, where g_{HH} and g_e are, respectively, the heavy-hole and elec-

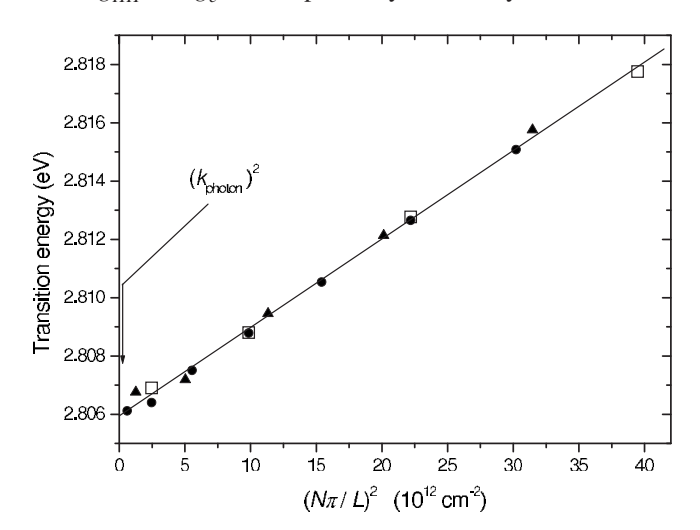


FIG. 2. Line positions of the c.m. excitonic features in the PL spectra from the three specimens, plotted against $(N\pi/L)^2$ [see Eq. (1)]. Open squares, filled triangles, and filled circles refer, respectively, to well widths of 20.7, 29.4, and 43.7 nm.

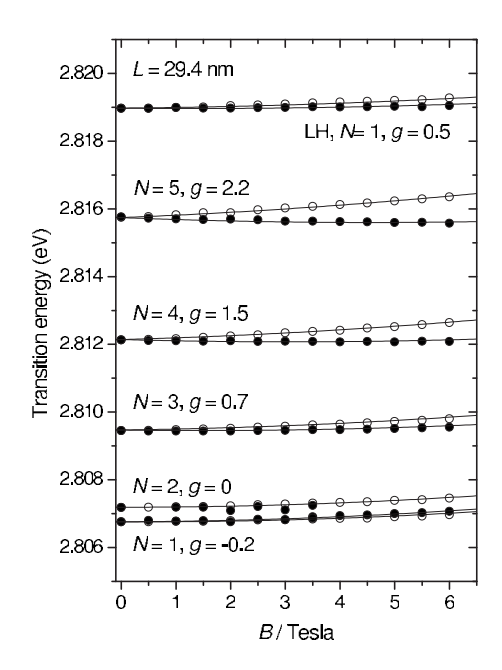


FIG. 3. Line positions of the c.m. excitonic signals in the PL spectra from the specimen with well width 29.4 nm as functions of a magnetic field applied in the growth direction. The continuous lines are of the form given in [Eq. (2)]. The open and filled symbols refer, respectively, to σ_+ and σ_- polarization of the emitted light.

tron g values for this field orientation. However, from Fig. 1(b), it is clear that, for fields along the growth direction, the Zeeman splittings, and hence the values of $g_{\rm exc}$, increase with the value of N. This can be seen more clearly in the fan diagram of Fig. 3 (where field dependent contributions to the energies due to diamagnetic shifts are also apparent). The continuous lines are on the form

$$E = E_N + DB^2 \pm g_{\rm exc} \mu_B B/2. \tag{2}$$

The term DB^2 describes the diamagnetic shift in the exciton line. For a given specimen, E_N , $g_{\rm exc}$, and D are functions of N.

Similar fan diagrams were obtained for the other two specimens and the corresponding values of $g_{\rm exc}$ are given in Table I. The diamagnetic shifts are too small to be measured accurately, but approximate values of the parameter D are also given in Table I.

In Refs. 1 and 2, it was pointed out that, when the values of $g_{\rm exc}$ for a series of quantum wells are considered, it is not the values of the quantum numbers N that are important: rather, what matter are the values of the z component of the translational wave vector. When the values of $g_{\rm exc}$ for the three samples are plotted (see Fig. 5 of Sec. III) on the same graph as functions of $K_z(=N\pi/L)$, they lie on a common curve, as was the case for a series of CdTe quantum wells.^{1,2} The explanation of this is given in Sec. III. In consequence, we write

$$g_{\text{exc}} = [g_{HH} + g(K_z)]\cos \theta - g_e, \tag{3}$$

where $g(K_z)$ is a function of K_z and where the field is at an angle θ to the growth direction. The $\cos \theta$ factor arises because the heavy-hole g value makes a contribution $g_{HH}\cos \theta$

TABLE I. Values of $g_{\rm exc}$ for different values of N used to fit the c.m. exciton transition energies as a function of magnetic field applied along the z axis. The accuracies of the values of $g_{\rm exc}$ are typically ± 0.10 . The values of the diamagnetic parameter D for θ =0 are $8.0\pm0.5\times10^{-6}$ eV T⁻² for entries in bold type and $7.0\pm0.5\times10^{-6}$ eV T⁻² for those in normal type. For θ =90°, the values of D are approximately 4×10^{-6} eV T⁻².

L	θ =0			θ=90°		
(nm)	20.7	29.4	43.7	20.7	29.4	43.7
N=1	-0.21	-0.20				
N=2	0.51	0	-0.08	-1.11		
N=3	1.38	0.72	0.23	-1.37	-1.29	-1.13
N=4	2.24	1.50	0.66			-1.13
N=5		2.20	1.17			-1.20
N=6			1.68			-1.29
N=7			2.09			

to $g_{\rm exc}$, ¹⁵ while it is shown in Ref. 2 (see also Sec. III below) that the contribution from the K_z -dependent term has a cos θ form. In contrast, the electron contribution is almost isotropic. ¹⁶

Figure 4 shows the dependence of $g_{\rm exc}$ on θ for some of the exciton transitions in the sample with L=43.7 nm, and confirms the expected behavior. In particular, when the magnetic field is perpendicular to the growth direction, the energy splittings are now only slightly dependent on the values of N [Fig. 1(c)]; in this arrangement, in which PL emitted

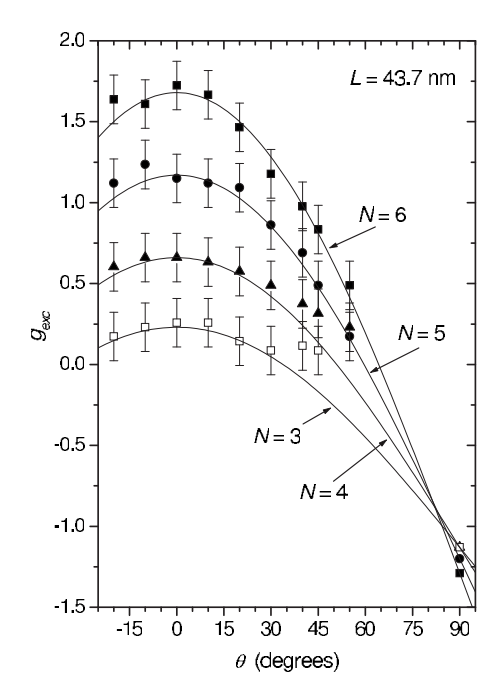


FIG. 4. Exciton g values for the specimen with well width 43.7 nm as a function of the angle θ between the magnetic field and the growth direction for the N=3 (open squares), N=4 (filled triangles), N=5 (filled circles), and N=6 (filled squares) transitions. The continuous lines are of the form of Eq. (3) with the parameters of Table I.

along the growth direction was monitored, the emitted light is unpolarized and the transitions cannot be separated by circular polarization analysis). The values of $g_{\rm exc}$ (Table I) now correspond approximately to the g-value of an electron (in bulk material g_e =1.12,^{17,18} and in strained material with S=13 meV, when θ =90°, $g_e \approx 1.15$).¹⁶

III. MODEL AND APPLICATION TO ZnSe

We shall see that the origin of the K_z -dependence of $g_{\rm exc}$ is due to mixing between the 1*S*-like heavy-hole exciton ground state and the higher lying *P*-like *light-hole* exciton states. The mixing is a result of the terms in the valence band Hamiltonian which cause the dispersion to depart from simple parabolic form. This Hamiltonian can be written, following Luttinger, ¹⁴ as

$$-H^{(v)}(\vec{\mathbf{k}}) = \left(\gamma_1 + \frac{5}{2}\gamma_2\right) \frac{\hbar^2 k^2}{2m_0} - \gamma_2 \frac{\hbar^2}{m_0} (k_x^2 J_x^2 + k_y^2 J_y^2 + k_z^2 J_z^2)$$

$$-2\gamma_3 \frac{\hbar^2}{m_0} (\{k_x k_y\} \{J_x J_y\} + \text{cycl.perm.}) - 2\mu_B \kappa \vec{J} \cdot \vec{B}$$

$$-2\mu_B q (B_x J_x^3 + B_y J_y^3 + B_z J_z^3), \tag{4}$$

where $\vec{\mathbf{k}}$ is the wave vector of the hole and $\{J_xJ_y\}$ = $\frac{1}{2}(J_xJ_y+J_yJ_x)$ etc. The directions x, y, z refer to the crystal [100], [010], and [001] axes. The quantities γ_1 , γ_2 , γ_3 , κ , and q are the (dimensionless) Luttinger parameters; m_0 is the electron rest mass; we shall assume that κ is much larger than q, so that the heavy-hole g value is given by $g_{HH} \approx -6\kappa$. The electron-hole exchange interaction has been omitted from Eq. (4) since it is small [about 0.4 meV (Ref. 19)] and in any case does not affect the Zeeman splittings for θ =0.

When dealing with excitons in the c.m. approximation, it is convenient⁶⁻⁸ to replace $H^{(v)}(\vec{\mathbf{k}})$ by $H^{(v)}(-\vec{\mathbf{p}}/\hbar + e\vec{\mathbf{A}}/\hbar + \beta\vec{\mathbf{K}})$. Here, (for $\vec{\mathbf{B}}$ along z), $\vec{\mathbf{p}}$ is the momentum operator for the electron within the exciton (equal to minus that of the hole) and $\beta = m_{HH}/(m_e + m_{HH})$, where m_e and m_{HH} are, respectively, the electron and heavy-hole effective masses. The vector potential $\vec{\mathbf{A}}$ is given⁶⁻⁸ by $\frac{1}{2}\vec{\mathbf{B}} \times \vec{\mathbf{r}}$, where $\vec{\mathbf{r}}$ is the electron-hole separation.

For general directions of the magnetic field and of the translational wave vector, the presence of the terms that involve γ_2 and γ_3 makes it impossible to separate the center of mass and internal motions, so that the hydrogenic envelope functions become mixed (this point will be discussed in detail elsewhere).²⁰ For the particular case of (001) wells, it is the terms that involve γ_3 that lead to the changes in the exciton g value.²

As a result, it is shown in Ref. 2 that the 1S HH ground states with $m_s = \pm 1/2$ and $m_J = \pm 3/2$ are mixed with nP states with $m_s = \pm 1/2$, $m_J = \pm 1/2$, and $m_l = \pm 1$, where m_l is the orbital quantum number. The matrix elements involved are on the form $|M_{\pm}| = (a \pm bB \cos \theta) K_z$, respectively, where a and b are both proportional to γ_3 [see Eq. (5) of Ref. 2]. The energies of the ground states are depressed by amounts $(a \pm bB \cos \theta)^2 K_z^2 / \Delta E_2$, where ΔE_n is the energy difference between the unperturbed nP LH and 1S HH state, given by

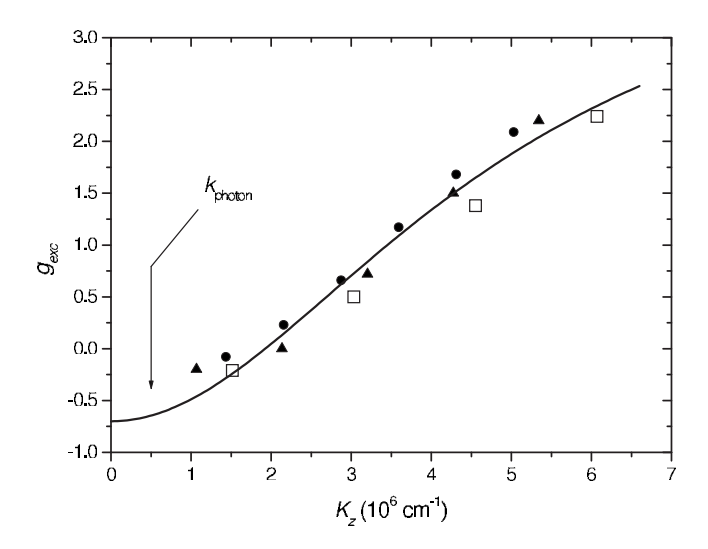


FIG. 5. $g_{\rm exc}$ vs K_z for the three specimens. Open squares, filled triangles, and filled circles refer, respectively, to well widths of 20.7, 29.4, and 43.7 nm, respectively. The continuous line is the predicted behavior for a value of γ_3 =0.97 and the other parameters given in the text.

$$\Delta E_n = \left(1 - \frac{1}{n^2}\right) + S + \hbar^2 \left(\frac{1}{2M_{BH}} - \frac{1}{2M_{BH}}\right) K_z^2.$$
 (5)

The presence of the cross terms linear in B thus leads² to contributions to the g value of

$$\delta g_1 = \left(\frac{24\gamma_3^2\hbar^2\beta^2\cos\theta}{m_0}\right) \left(\frac{v_n w_n}{\Delta E_n}\right) K_z^2,\tag{6}$$

where $v_n = -\langle nP, p_x | \partial / \partial x | 1S \rangle a_{\text{exc}}$ and $w_n = \langle nP, p_x | x | 1S \rangle a_{\text{exc}}^{-1}$.

There are similar contributions from all nP states, including P-like states in the continuum.² For the present ZnSe layers, for which the strain splitting S=13 meV, we take $\gamma_1=2.45$, $\gamma_2=0.61$, 21 R=20 meV, 12 and $m_e=0.145m_0$. ¹⁹ To fit the extrapolated value for $g_{\rm exc}$ for $\theta=0$ at a notional value of $K_z=0$, we take $g_e=1.12$ (Refs. 17 and 18) and $g_{HH}=0.42\pm0.20$. The calculated curve for these values is shown in Fig. 5 and produces excellent agreement with experiment with a value of $\gamma_3=0.98\pm0.05$, which compares with the value of 1.11 ± 0.11 from Ref. 21. The value of g_{HH} corresponds to $\kappa\approx-0.07$ in Eq. (4).

When the field is at a right angle to the growth direction $(\theta=90^\circ)$, there are no contributions to the exciton g value due to the mixing [see Eq. (6)] and the heavy-hole g value also becomes zero. As a result, the exciton g value becomes equal in magnitude to that of the electron, as is observed experimentally as in Fig. 4 [see also Table I; the sign of $g_{\rm exc}$ changes as θ goes to 90° , in accordance with Eq. (3)]. For the higher lying states in the well, the magnitude of g_e is seen (Table I) to become significantly larger than the bulk ZnSe value of 1.12. This is ascribed to the finite depth of the quantum well and penetration of the wave functions into the barrier regions, as discussed in Ref. 16.

In the three specimens, we have also been able to determine the values of $g_{\rm exc}$ for the N=1 light-hole states, the values being on the order of 0.5. These values will be af-

fected both by the proximity of the relevant part of the dispersion curve to the region where polariton effects are important and, as for the heavy holes, by motion-induced mixing with other excited states. Calculation of these parameters is, however, beyond the scope of the present article.

The terms in $|M_{\pm}|^2$, which involve B^2 , lead to K_z -dependent negative contributions to the diamagnetic shifts. These contributions contain the factor $a_{\rm exc}^2$. We take $a_{\rm exc}=3.5$ nm and find that, at the highest value of K_z ($6\times 10^6~{\rm cm}^{-1}$) that could be studied, the decrease (relative to the value at $K_z=0$) in the diamagnetic parameter D due to the mixing is calculated to be $9\times 10^{-7}~{\rm eV}~{\rm T}^{-2}$ This is at the limit of experimental detection, but is in agreement with the decrease on order $10^{-6}~{\rm eV}~{\rm T}^{-2}$ given in Table I. In the case of CdTe, the much larger exciton Bohr radius [\$\approx 7.2~{\rm nm}~{\rm (Ref.~2)}] allowed this motion-dependent decrease in D to be much more clearly observable.

IV. CONCLUSIONS

The observations above provide strong confirmation that the magnetic properties of excitons are affected strongly as they acquire kinetic energy. In the center of mass approximation, the origin of the effect is motion-induced mixing between the 1S exciton ground state and excited states of nP form. The mixing is caused by the γ_3 terms in the description of the valence band dispersion curve. In the case of CdTe, a model for this process led to a successful quantitative description of the motion-induced changes in the magnetic mo-

ments and of the diamagnetic shifts. As a consequence, the magnetic moment of the exciton is not simply the sum of the magnetic moments of the electron and hole, but contains motion-induced contributions, which can easily dominate the contributions from the individual charge carriers.

In the present paper, we have shown that this model accounts equally well for the detailed properties of a second semiconductor, ZnSe, with a value of γ_3 of 0.98 ± 0.05 for the Luttinger parameter γ_3 in excellent agreement with the value of 1.11 ± 0.11 determined from two-photon magnetoabsorption spectra.²¹ ZnSe differs from CdTe is several respects: in particular, the signs of the g values of the individual charge carriers in ZnSe are opposite to those in CdTe. The combined data for the two materials thus show unequivocally that it is the motion-induced mixing process that leads to the observed changes in the exciton g value, rather than, for example, quantum confinement changes in the g values of the individual electrons and holes. In other words, the behavior is characteristic of the exciton as a whole, rather than of its constituent particles. The success of the model in describing the properties of these two different semiconductors thus provides convincing evidence for the universality of motion-induced changes in exciton magnetism.

ACKNOWLEDGMENTS

We are grateful for support from the EPSRC (U.K.) (Project No. EP/E025412), the Royal Society, the RFBR, the Presidium RAS, and the German Research Foundation DFG within Project No. Ho1388/28 (A.G.).

^{*}j.j.davies@bath.ac.uk

¹J. J. Davies, D. Wolverson, V. P. Kochereshko, A. V. Platonov, R. T. Cox, J. Cibert, H. Mariette, C. Bodin, C. Gourgon, E. V. Ubyivovk, Yu. P. Efimov, and S. A. Eliseev, Phys. Rev. Lett. **97**, 187403 (2006).

²L. C. Smith, J. J. Davies, D. Wolverson, S. Crampin, R. T. Cox, J. Cibert, H. Mariette, V. P. Kochereshko, M. Wiater, G. Karczewski, and T. Wojtowicz, Phys. Rev. B 78, 085204 (2008).

³ V. P. Kochereshko, L. C. Smith, J. J. Davies, R. T. Cox, A. Platonov, D. Wolverson, H. Boukari, H. Mariette, J. Cibert, M. Wiater, T. Wojtowicz, and G. Karczewski, Phys. Status Solidi B 245, 1059 (2008).

⁴V. P. Kochereshko, A. Platonov, D. Loginov, J. J. Davies, D. Wolverson, L. C. Smith, H. Boukari, R. T. Cox, J. Cibert, and H. Mariette, Semicond. Sci. Technol. 23, 114011 (2008).

⁵J. J. Davies, L. C. Smith, D. Wolverson, H. Boukari, R. T. Cox, H. Mariette, J. Cibert, and V. P. Kochereshko, J. Korean Phys. Soc. 53, 2803 (2008).

⁶J. O. Dimmock, in *Semiconductors and Semimetals*, edited by R. K. Willardson and A. C. Beer (Academic, New York, 1967), Vol. 3, p. 259

⁷M. Altarelli and N. O. Lipari, Phys. Rev. B **7**, 3798 (1973).

⁸ K. Cho, S. Suga, W. Deybrodt, and F. Willman, Phys. Rev. B 11, 1512 (1975).

⁹E. L. Ivchenko and G. Pikus, *Superlattices and Other Microstructures* (Springer-Verlag, Berlin, 1995).

¹⁰E. L. Ivchenko, *Semiconductor Nanostructures* (Alpha Science International, Harrow, UK, 2005).

¹¹ S. Schumacher, G. Czycholl, F. Jahnke, I. Kudyk, H. I. Rückmann, J. Gutowski, A. Gust, G. Alexe, and D. Hommel, Phys. Rev. B 70, 235340 (2004).

¹²J. Gutowski, K. Sebald, and T. Voss, in *Semiconductors: New Data and Updates for II-VI Compounds*, Landolt-Börnstein, New Series, Group III, Vol. 44, edited by U. Roessler (Springer-Verlag, Berlin, 2008).

¹³S. Lankes, M. Meier, T. Reisinger, and W. Gebhardt, J. Appl. Phys. **80**, 4049 (1996).

¹⁴J. M. Luttinger, Phys. Rev. **102**, 1030 (1956).

¹⁵e.g., J. L. Patel, J. E. Nicholls, and J. J. Davies, J. Phys. C **14**, 1339 (1981).

¹⁶J. J. Davies, D. Wolverson, I. J. Griffin, O. Z. Karimov, C. L. Orange, D. Hommel, and M. Behringer, Phys. Rev. B 62, 10329 (2000).

¹⁷J. E. Nicholls, J. J. Davies, N. R. J. Poolton, R. Mach, and G. O. Müller, J. Phys. C **18**, 455 (1985).

¹⁸D. J. Dunstan, J. E. Nicholls, B. C. Cavenett, and J. J. Davies, J. Phys. C **13**, 6409 (1980).

¹⁹N. Miura, Y. Imanaka, and H. Nojiri, Mater. Sci. Forum **182-184**, 287 (1995).

²⁰V. P. Kochereshko (unpublished).

²¹ H. W. Hölscher, A. Nöthe, and Ch. Uihlein, Phys. Rev. B 31, 2379 (1985).